Changes in cell fate determine the regenerative and functional capacity of the developing kidney before and after release of obstruction

Vidya K. Nagalakshmi[1], Minghong Li[1], Soham Shah[2], Joseph C. Gigliotti[3], Alexander L. Klibanov[4], Frederick H. Epstein[2], Robert L. Chevalier[1], R. Ariel Gomez[1] and Maria Luisa S. Sequeira-Lopez [1†]

[1] Department of Pediatrics, University of Virginia School of Medicine, Charlottesville, VA

[2] Department of Biomedical Engineering, University of Virginia Health System, Charlottesville, VA

[3] Department of Integrated Physiology and Pharmacology, Liberty University College of Osteopathic Medicine, Lynchburg, VA

[4] Cardiovascular Division, University of Virginia Health System, VA

† Corresponding author:

Running Title: Cell Fate Change And Kidney Injury

Maria Luisa S. Sequeira Lopez, M.D.

Professor of Pediatrics

University of Virginia School of Medicine

409 Lane Rd MR4 Bldg room 2001

Charlottesville, VA 22908

msl7u@virginia.edu

Phone: 434-924-5065

Fax: 434-982-4328

Key words: Obstructive nephropathy, lineage tracing, renal progenitors, nephrovascular development and kidney regeneration

Figure S1

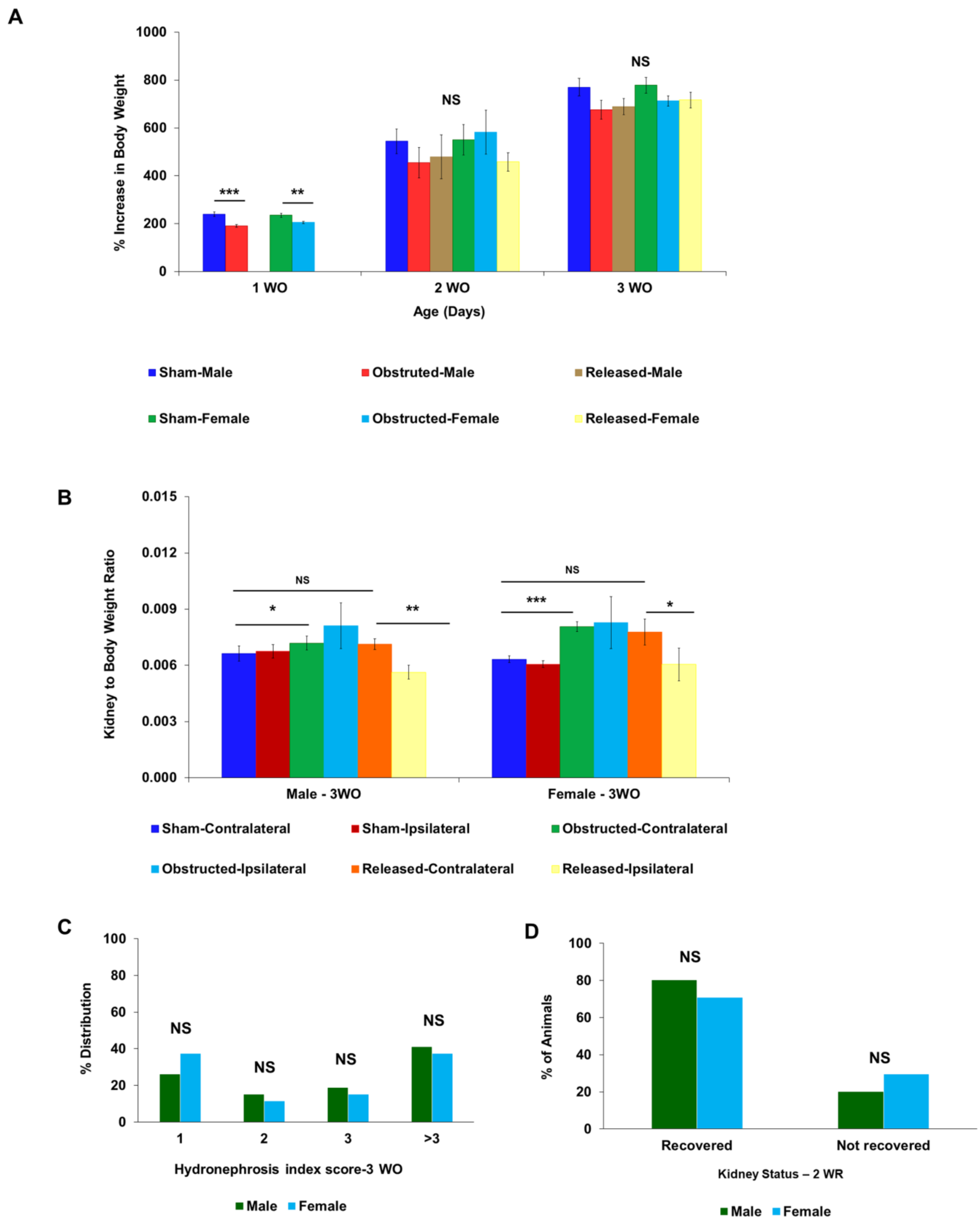
A
% Increase in Body Weight
1000
800
600
400
200
0
***
**
NS
NS
1 WO
2 WO
3 WO
Age (Days)
Sham-Male
Obstruted-Male
Released-Male
Sham-Female
Obstructed-Female
Released-Female
B
Kidney to Body Weight Ratio
0.015
0.012
0.009
0.006
0.003
0.000
NS
*
**
NS
***
*
Male - 3WO
Female - 3WO
Sham-Contralateral
Sham-Ipsilateral
Obstructed-Contralateral
Obstructed-Ipsilateral
Released-Contralateral
Released-Ipsilateral
C
% Distribution
100
80
60
40
20
0
NS
NS
NS
NS
1
2
3
>3
Hydronephrosis index score-3 WO
Male
Female
D
% of Animals
100
80
60
40
20
0
NS
NS
Recovered
Not recovered
Kidney Status – 2 WR
Male
Female

Figure S1. Morphometric changes during obstruction and post-release: (A). Change in body weight following surgery: At 1 week post-obstruction, body weight gain was decreased in obstructed animals (Male: n=62; Female: n=57) compared to sham-operated animals (Male: n=31; Female: n=30). No significant differences were observed at 2 and 3 weeks post-surgery. (B) A significant increase was seen in the contralateral kidneys in obstructed animals (males and females) in comparison to contralateral kidneys of shams. No significant differences were observed in the kidney-to-body weight ratio of contralateral kidneys following the release of obstruction in comparison to sham-operated animals. Sham operated (Male: n=16 Female: n=18), obstructed (Male: n= 27 Female: n=28) and released (Male: n= 18 Female: n=12; $^{*}P< 0.05$; $^{**}P<0.01$; $^{***}P<0.001$). (C and D) No significant differences were observed in the hydronephrosis score between males (n=27) and females (n=27) observed at 3 weeks post obstruction. Similarly, the extent of recovery was not significantly different between males (n= 25) and females (n=17) following the release of obstruction.

Figure S2

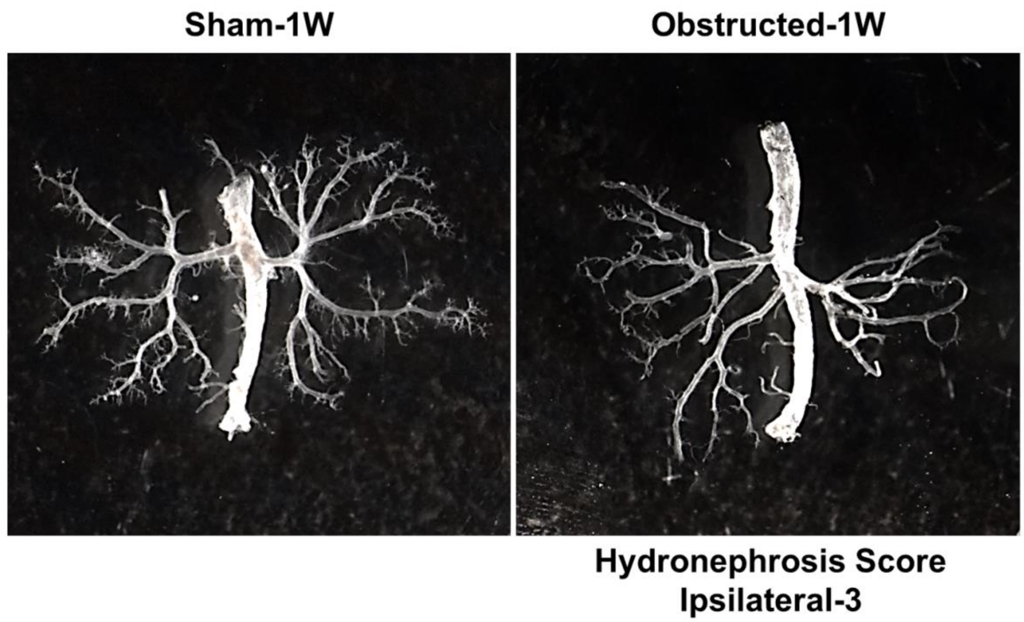

Figure S2. Vascular damage at 1 week post-obstruction: Arterial microdissection at one week post obstruction revealed a decreased arteriolar branching in the obstructed kidneys. In addition to the damage observed in the ipsilateral kidneys, contralateral kidneys also showed a marked decrease in arteriolar branching.

Figure S3

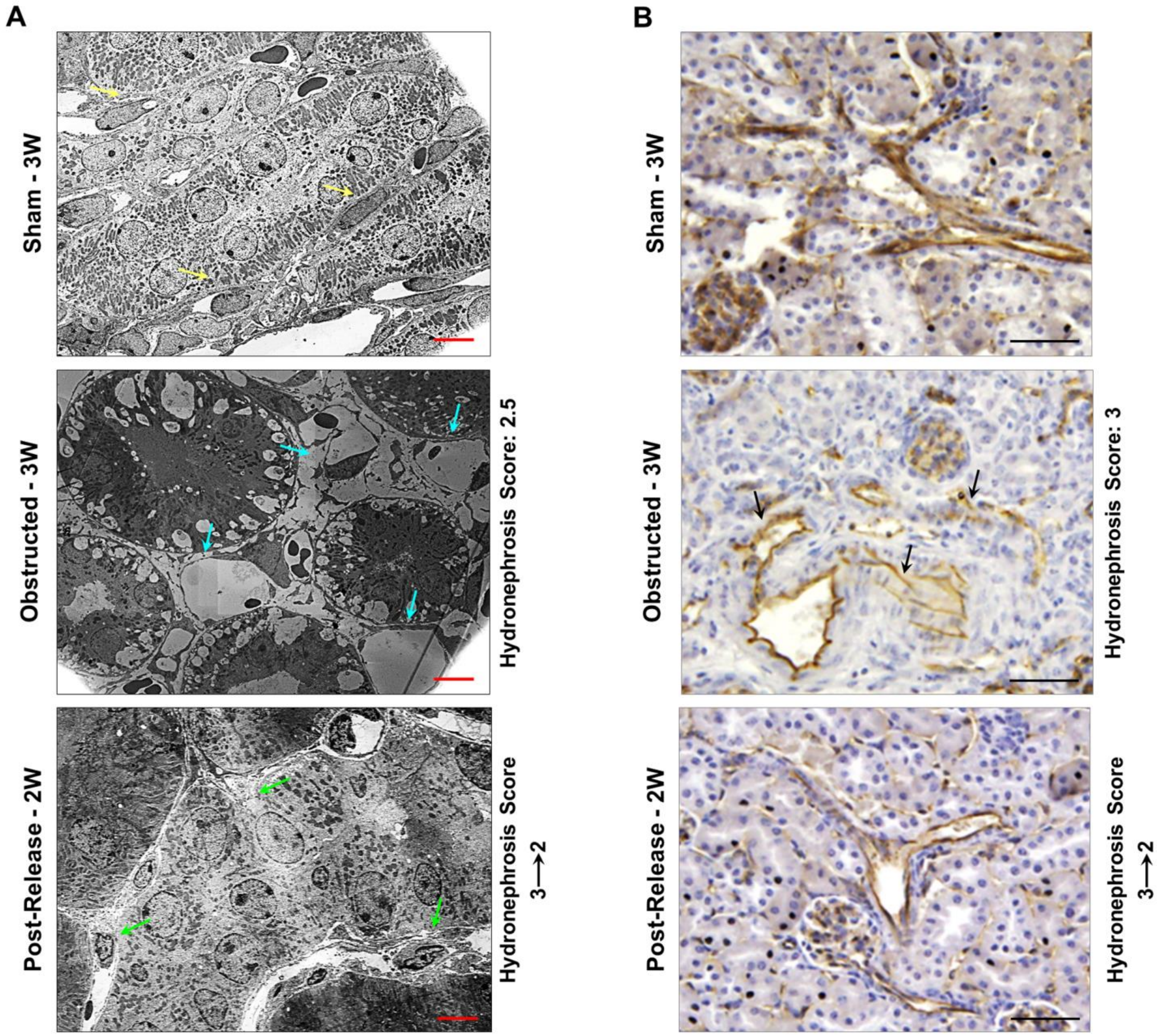

Figure S3: Vascular rarefaction and loss of endothelial cell Integrity during obstruction injury and recovery following relief of obstruction: (A) STEM images on kidneys from 3W obstructed animals showed extensive degeneration of the renal vasculature accompanied with capillary lumen dilation and loss of pericytes and smooth muscle cells (Cyan arrows). A remarkable recovery in the endothelial lining of the renal microvasculature is observed post-release of obstruction. Extensive vascular repair and regeneration subsequent to the release of obstruction resulted in the restoration of vascular structures (green arrows) similar to sham-operated kidneys (yellow arrows). Scale bars, 5µm (B). PECAM staining shows loss of renal interstitial capillaries and vascular rarefaction (arrows) after obstruction for 3 weeks. Release of obstruction brings forth a significant repair of the vasculature as indicated by an endothelial staining pattern similar to sham-operated kidneys. Scale bars, 20µm.

Figure S4

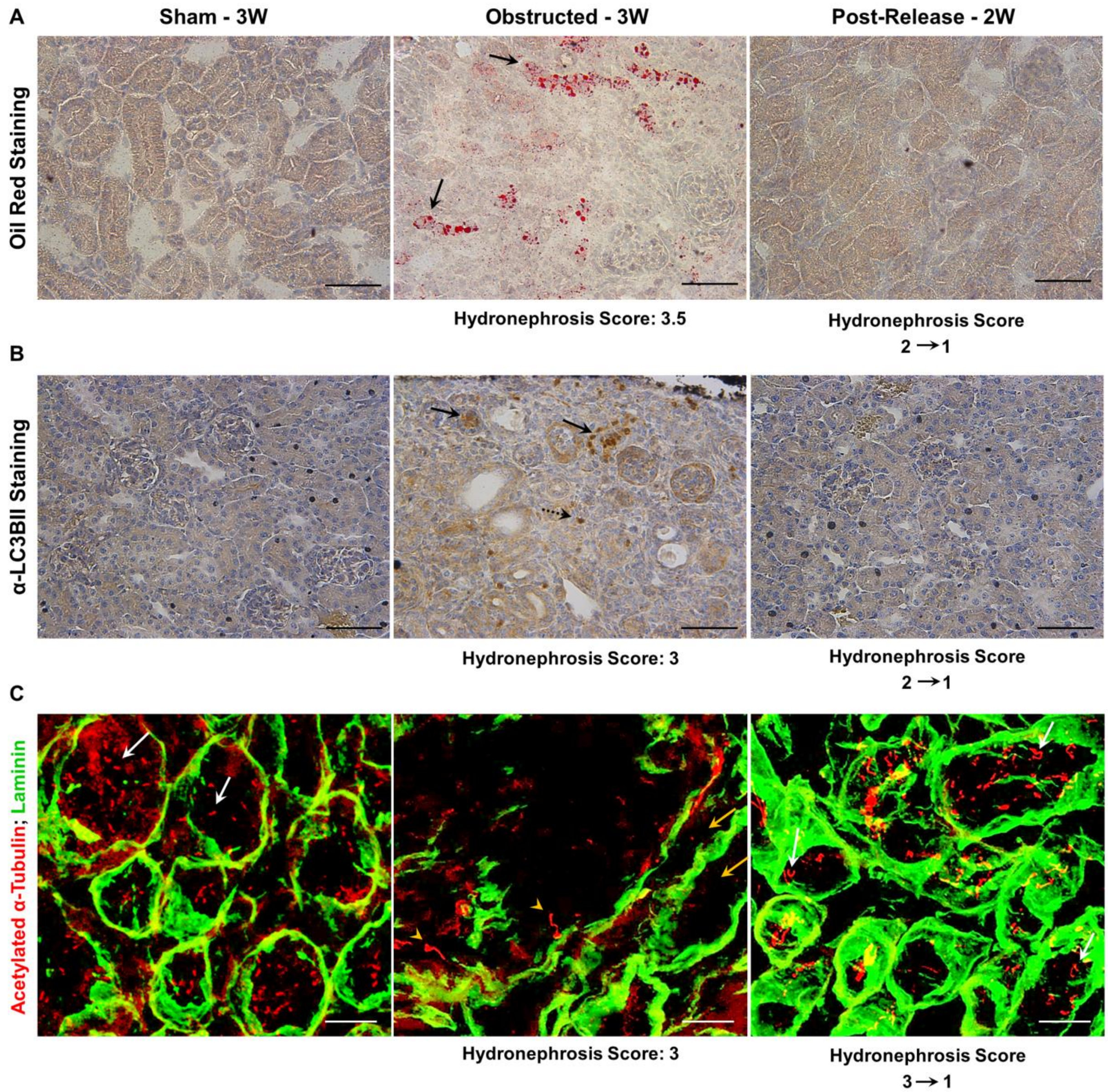

Figure S4. Relief of obstruction ameliorates tubular damage due to obstruction: (A) Oil red staining on kidney sections displayed an increased lipid accumulation in the tubules after persistent 3W of obstruction (black arrows) in comparison to sham kidneys. Following the release of obstruction, lipid accumulation in the damaged tubules decreased (Scale bars, 50µm). **(B)** Expression of the autophagic marker LC3B-II increased in damaged tubular (black arrows) and interstitial cells (dashed arrow) in the 3W obstructed kidneys compared to sham kidneys. Release of obstruction prevented the abnormal increase in autophagy. Scale bars, 50µm. **(C)** Acetylated alpha tubulin staining marks the intact primary cilium in laminin positive renal tubular epithelium as seen in sham kidneys (white arrows). In 3W obstructed kidneys, the primary cilium undergoes changes, being long in some tubular cells (yellow arrow heads) and absent in the damaged and degenerating tubules (yellow arrows). The release of obstruction resulted in a remarkable regeneration of cilia in the tubular epithelium undergoing repair and remodeling (white arrows – post release 2W). Scale bars, 10 µm.

Figure S5

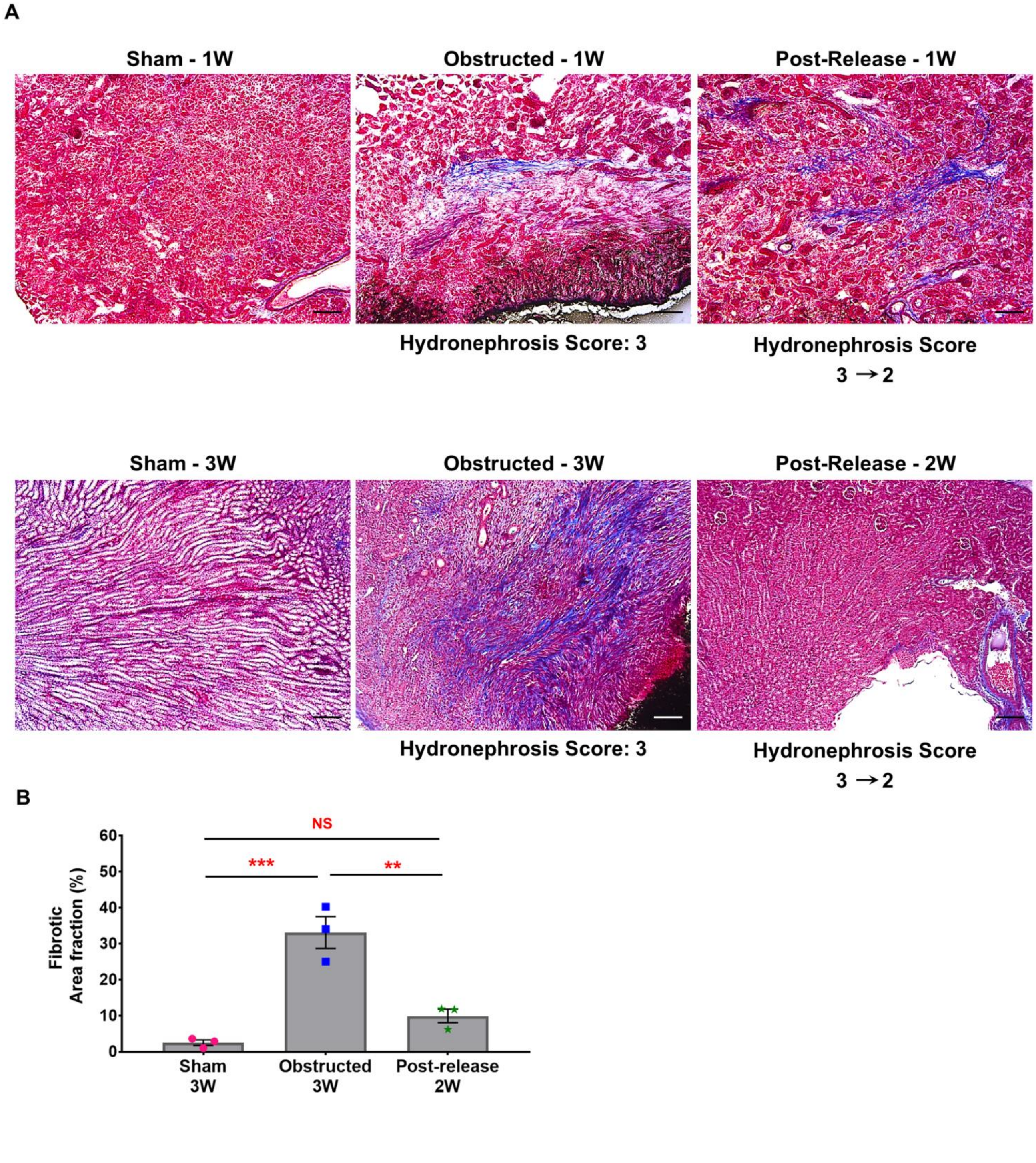

Figure S5. Interstitial fibrotic damage during pUUO and its recovery on release of obstruction: (A) Masson's Trichrome staining revealed an increase in interstitial collagen in obstructed kidneys (indicated by blue color) after 1 week when compared to sham kidneys of similar age groups. Release of obstruction resulted in partial recovery in the interstitial collagen deposition at 1 week post-release and a complete absence of interstitial collagen at 2W after release. Scale bars, 100 µm. (B) Quantification of collagen positive area revealed a significant increase in the obstructed kidneys at 3W (n=3) in comparison to sham kidneys (n=3). Released kidneys (n=3) presented a significant recovery in the collagen area and is restored to similar level as in the 3W sham (n=3) group (**$P<0.01$; ***$P<0.001$; NS-Non significant)

Figure S6

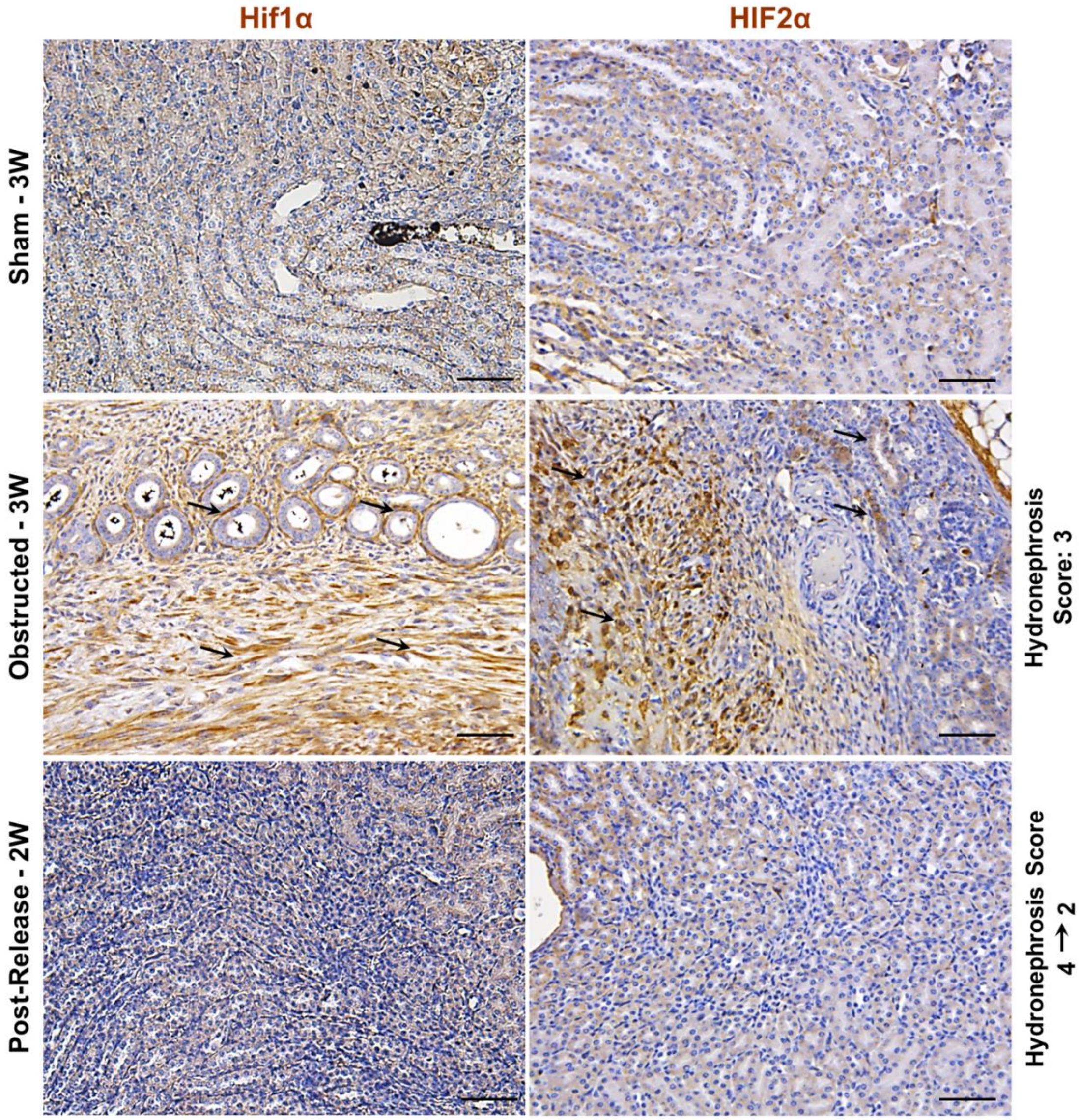

Figure S6. Hypoxia during severe obstruction injury: Immunostaining for hypoxia induced proteins Hif1α and Hif2α indicate increase in the expression of these proteins only in the severely damaged regions of the tissue sections collected from 3W obstructed kidneys. No obvious signals for Hif1α and Hif2α were observed in 3W sham and released kidneys at 2W post-release. Scale bars, 50µm.

Figure S7

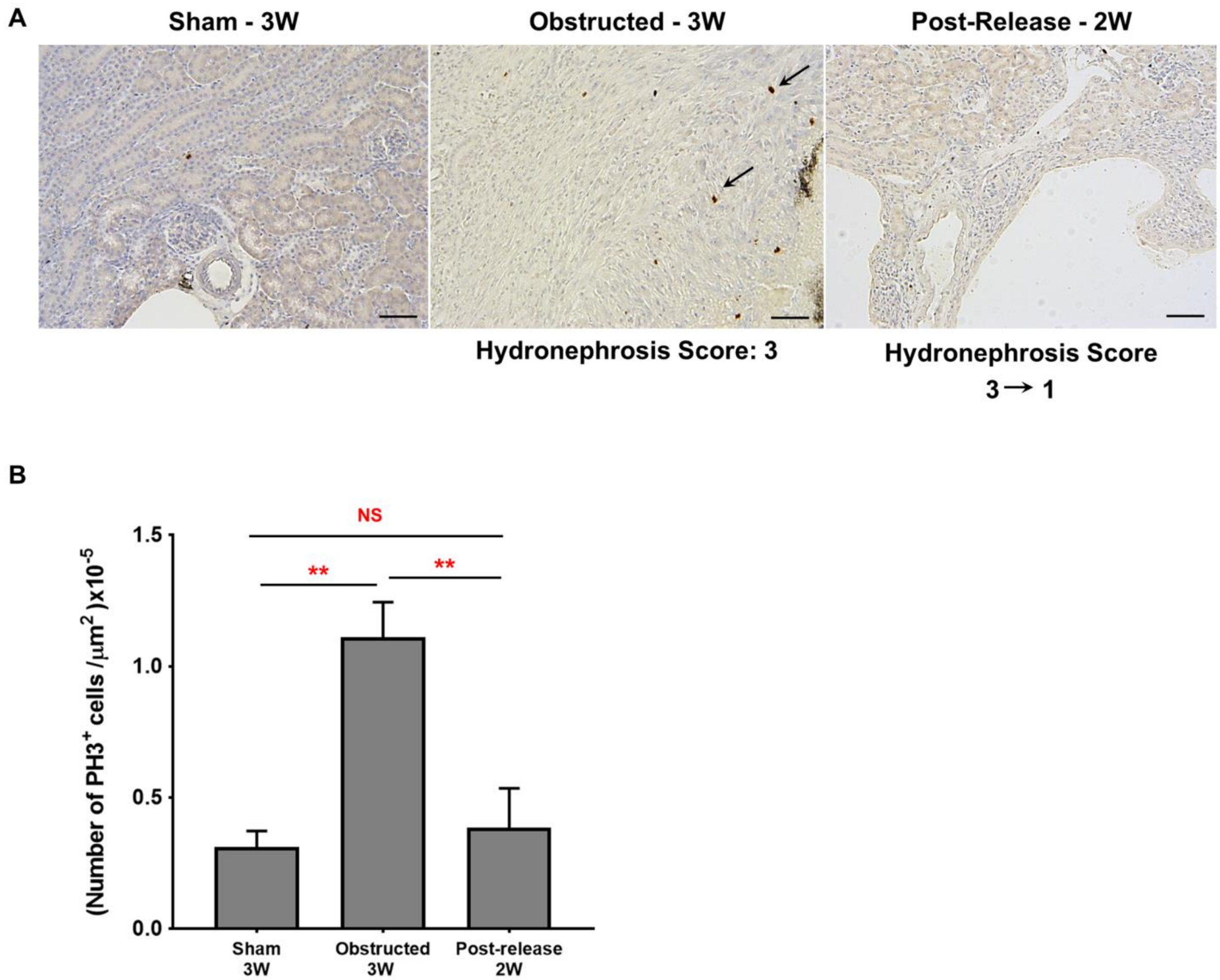

Figure S7. Increased cell proliferation during obstructive injury: (A) Mitotic index measured in 3W animals by immunostaining for phospho-histone H3 (PH3) showed a significant increase in $PH3^+$ proliferating cells during obstruction (black arrows) compared to sham-operated kidneys and a decrease to sham levels following the release of pUUO. Scale bars, 50μm. (B) Bar graph showing the quantification of $PH3^+$ proliferating cells in sham (n=3) obstructed (n=4) and post-released (n=3) kidneys. (***P*<0.01; NS-Non significant).

Figure S8

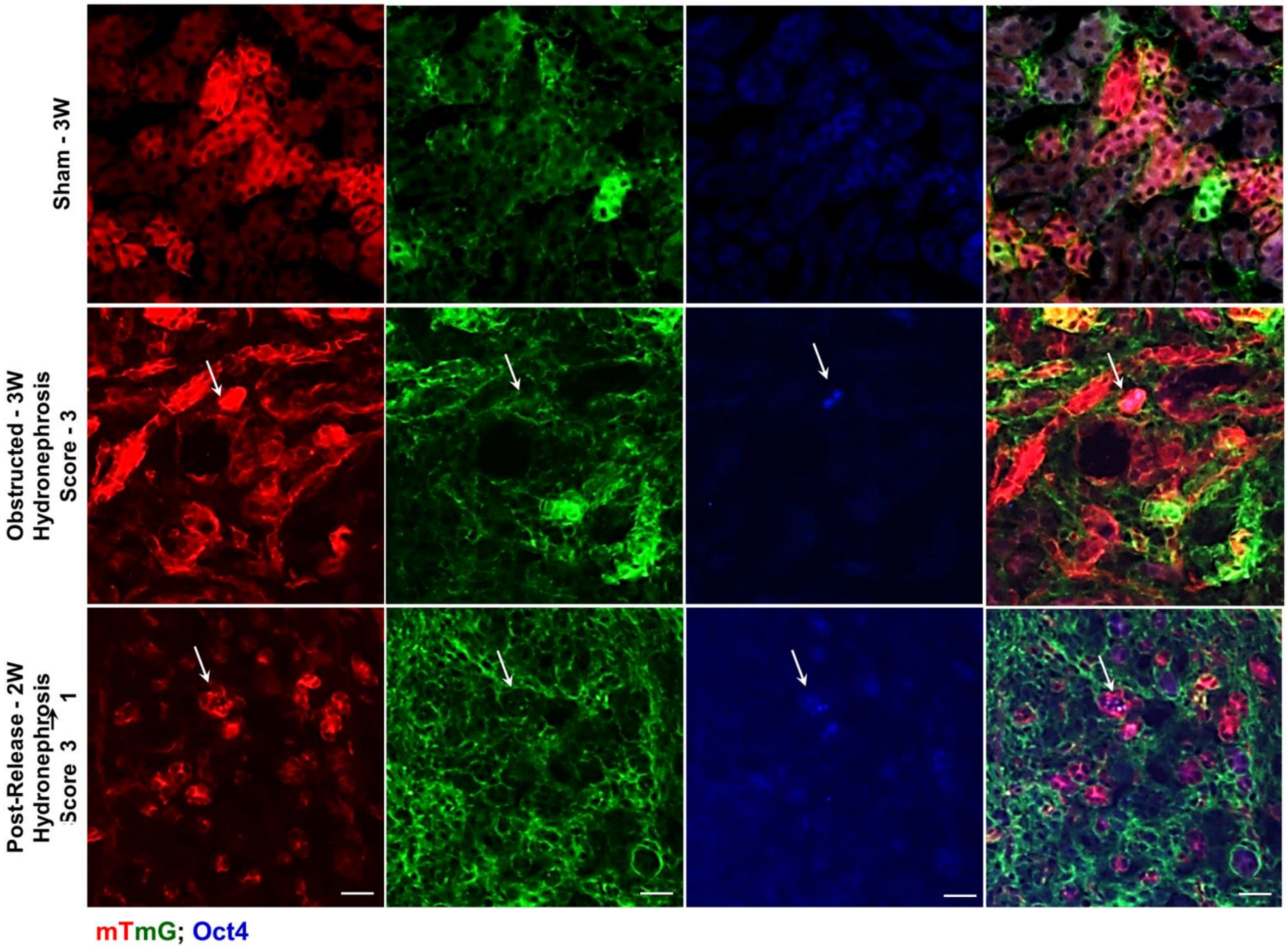

Figure S8. De-differentiation of adult renal cells during kidney injury and repair: Kidneys sections from 3W sham, obstructed and released animals from the *Foxd1.Cre; mTmG* cross were immunostained for the embryonic stem cell marker Oct4. Some of the double positive (GFP^+ and RFP^+) cells were also positive for Oct4 signals (white arrows) only in the obstructed and release groups. Scale bars, 20µm.

Figure S9

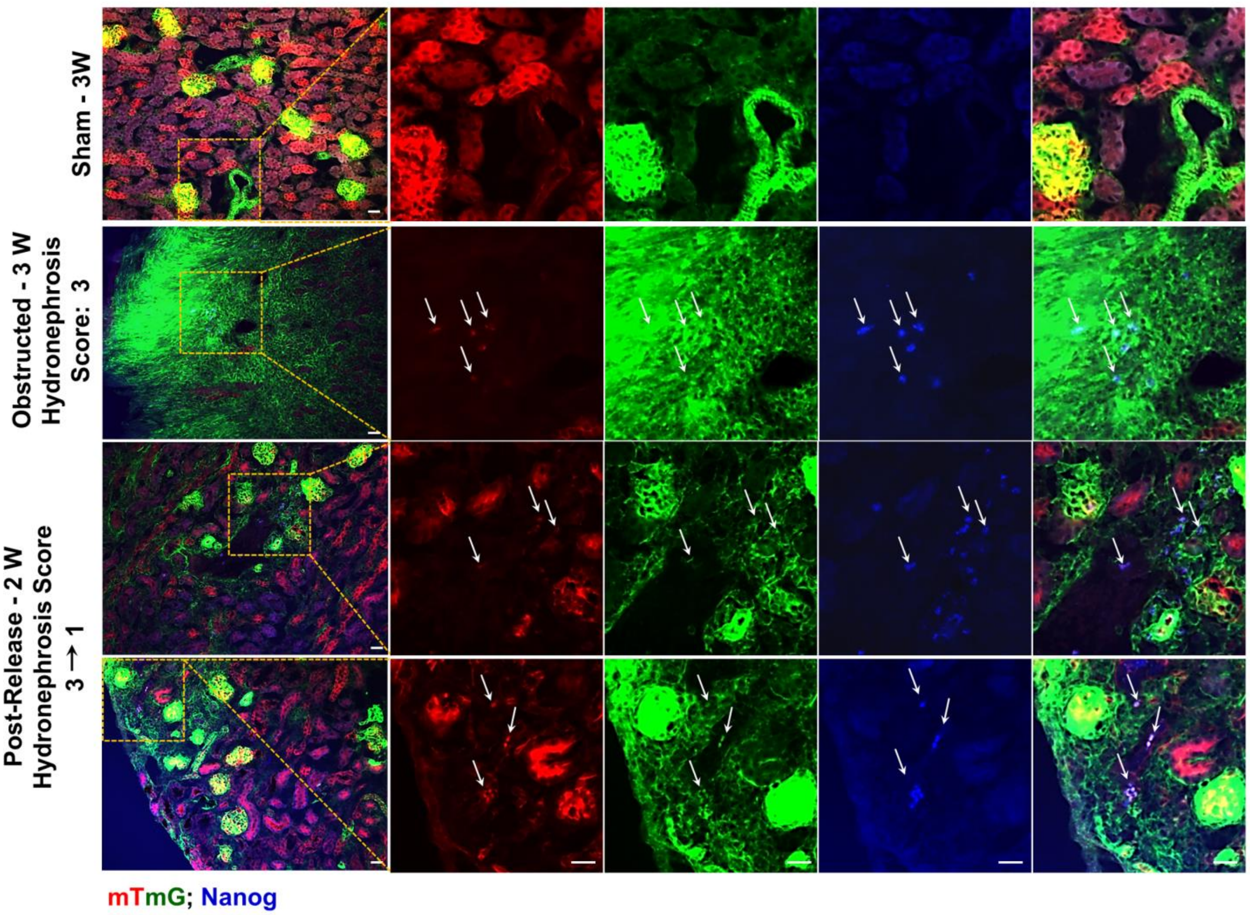

Figure S9. De-differentiation of adult renal cells during kidney injury and repair: Kidneys sections from 3W sham, obstructed and released animals from the *Foxd1.Cre;mTmG* cross were immunostained for the embryonic stem cell marker Nanog. Some of the double positive (GFP^+ and RFP^+) cells were also positive for Nanog signals (white arrows) only in the obstructed and release groups. Scale bars, 20µm.

Figure S10

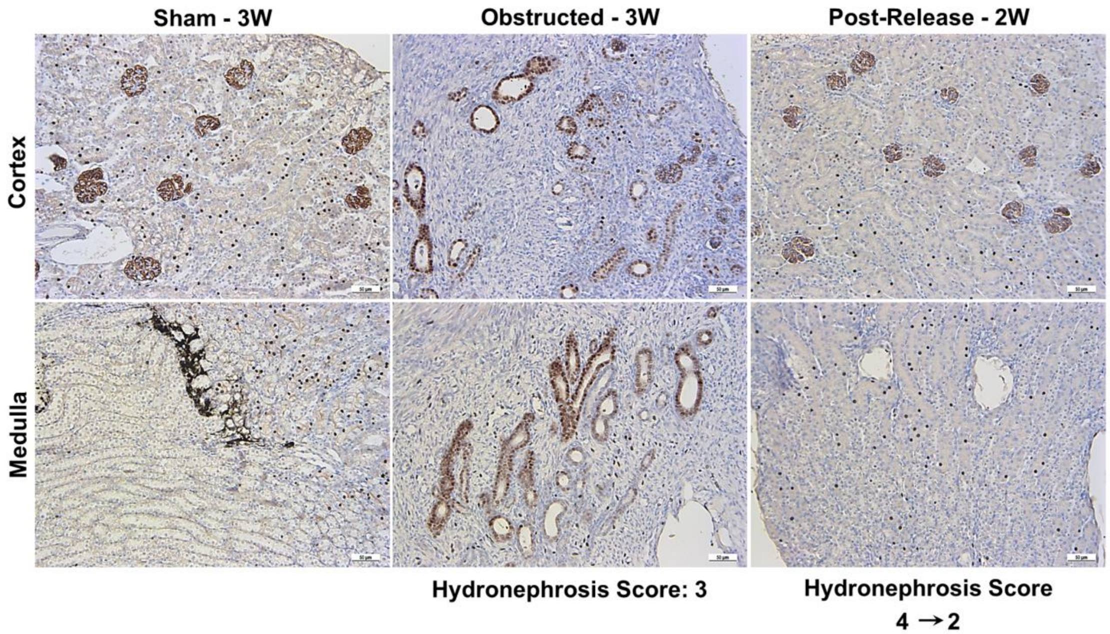

Figure S10. Changes in Sox9 expression during kidney injury and repair: Kidney sections from 3W obstructed animals revealed a significant increase in tubular Sox9 which marks pluripotent-like cells in the tubular epithelium. Two weeks following the release of obstruction, tubular Sox9 expression signals returned to levels not different from sham kidneys. Scale bars, 50µm.